RESEARCH ARTICLE

MicroRNA changes of bone marrow-derived mesenchymal stem cells differentiated into neuronal-like cells by Schwann cell-conditioned medium

Zhi-Jian Wei[1,#], Bao-You Fan[1,#], Yang Liu[1,#], Han Ding[1], Hao-Shuai Tang[1], Da-Yu Pan[1], Jia-Xiao Shi[1], Peng-Yuan Zheng[1], Hong-Yu Shi[1], Heng Wu[2], Ang Li[3], Shi-Qing Feng[1,*]

1 Department of Orthopedics, Tianjin Medical University General Hospital, Tianjin, China
2 Tianjin Key Laboratory of Lung Cancer Metastasis and Tumor Microenvironment, Tianjin Lung Cancer Institute, Tianjin Medical University General Hospital, Tianjin, China
3 Department of Orthopedics, Henan Provincial People's Hospital, Zhengzhou, Henan Province, China

Funding: *The present study was supported by the National Natural Science Foundation of China, No. 81330042, 81620108018 (both to SQF), and 81702147 (to ZJW).*

Graphical Abstract

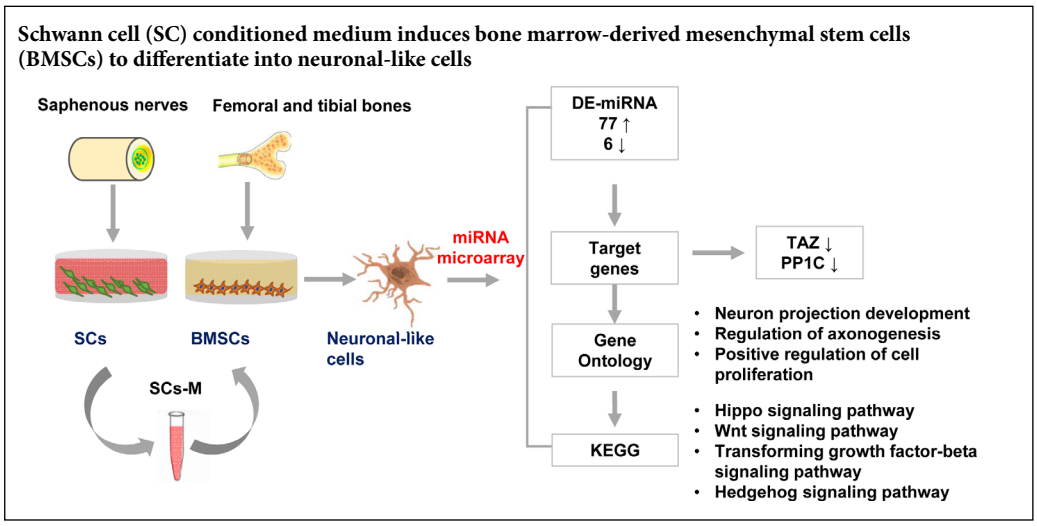

Correspondence to:
Shi-Qing Feng, MD,
sqfeng@tmu.edu.cn.

#These authors contributed equally to this study.

orcid:
0000-0001-9437-7674
(Shi-Qing Feng)

doi: *10.4103/1673-5374.253532*

Received: *June 30, 2018*
Accepted: *December 11, 2018*

Abstract

Bone marrow-derived mesenchymal stem cells differentiate into neurons under the induction of Schwann cells. However, key microRNAs and related pathways for differentiation remain unclear. This study screened and identified differentially expressed microRNAs in bone marrow-derived mesenchymal stem cells induced by Schwann cell-conditioned medium, and explored targets and related pathways involved in their differentiation into neuronal-like cells. Primary bone marrow-derived mesenchymal stem cells were isolated from femoral and tibial bones, while primary Schwann cells were isolated from bilateral saphenous nerves. Bone marrow-derived mesenchymal stem cells were cultured in unconditioned (control group) and Schwann cell-conditioned medium (bone marrow-derived mesenchymal stem cell + Schwann cell group). Neuronal differentiation of bone marrow-derived mesenchymal stem cells induced by Schwann cell-conditioned medium was observed by time-lapse imaging. Upon induction, the morphology of bone marrow-derived mesenchymal stem cells changed into a neural shape with neurites. Results of quantitative reverse transcription-polymerase chain reaction revealed that nestin mRNA expression was upregulated from 1 to 3 days and downregulated from 3 to 7 days in the bone marrow-derived mesenchymal stem cell + Schwann cell group. Compared with the control group, microtubule-associated protein 2 mRNA expression gradually increased from 1 to 7 days in the bone marrow-derived mesenchymal stem cell + Schwann cell group. After 7 days of induction, microRNA analysis identified 83 significantly differentially expressed microRNAs between the two groups. Gene Ontology analysis indicated enrichment of microRNA target genes for neuronal projection development, regulation of axonogenesis, and positive regulation of cell proliferation. Kyoto Encyclopedia of Genes and Genomes pathway analysis demonstrated that Hippo, Wnt, transforming growth factor-beta, and Hedgehog signaling pathways were potentially associated with neural differentiation of bone marrow-derived mesenchymal stem cells. This study, which carried out successful microRNA analysis of neuronal-like cells differentiated from bone marrow-derived mesenchymal stem cells by Schwann cell induction, revealed key microRNAs and pathways involved in neural differentiation of bone marrow-derived mesenchymal stem cells. All protocols were approved by the Animal Ethics Committee of Institute of Radiation Medicine, Chinese Academy of Medical Sciences on March 12, 2017 (approval number: DWLI-20170311).

Key Words: *nerve regeneration; microRNA analysis; bone marrow-derived mesenchymal stem cells; Schwann cells; neuronal-like cells; neuronal differentiation; Gene Ontology analysis; Hippo signaling pathway; Wnt signaling pathway; transforming growth factor-beta signaling pathway; Hedgehog signaling pathway; neural regeneration*

Chinese Library Classification No. *R453; R364*

Introduction

Bone marrow-derived mesenchymal stem cells (BMSCs), one source of mesenchymal stem cells (MSCs), have been applied medically for diverse indications ranging from bone regeneration to cardiac repair (Vaquero and Zurita, 2011; Garg et al., 2017). BMSCs have been documented as capable of differentiating into multiple cell types, such as osteoblasts, chondrocytes, myocytes, and adipocytes (Robey, 2017). Despite ongoing debates about the genuine functionality of these differentiated cells, interest in the neuronal differentiation or transdifferentiation (because they span different germinal layers) capacity of BMSCs has persisted (Venkatesh and Sen, 2016). Several studies have reported that neuron-like cells derived from BMSCs shared similar electrophysiological and functional characteristics with normal neurons (Song et al., 2007; Seo et al., 2018; Yang et al., 2018). Therefore, a proper induction strategy seems to be more important for specifying cell fate, regardless if it is a morphological mimic or bona fide neuron.

Neuronal induction methods for BMSCs include chemical agents such as butylated hydroxyanisole and dimethyl sulfoxide (Woodbury et al., 2000, 2002; Schultz and Lucas, 2006); or isobutylmethylxanthine, 5-azacytidine, β-mercaptoethanol, and retinoic acid (Deng et al., 2001; Hung et al., 2002); neurotrophic factors such as brain-derived neurotrophic factor, basic fibroblast growth factor, epidermal growth factor, or a combination of these factors (Tohill et al., 2004; Tzeng et al., 2004); and cell co-culture systems (Xu et al., 2017). However, others have argued that these methods only result in morphological changes that can also be elicited by other chemical stressors (Neuhuber et al., 2004; Bertani et al., 2005), and are a short-term phenomenon that will be reversed upon the withdrawal of agents (Zurita et al., 2008). An alternative differentiation strategy involves the use of co-culture or mixed culture conditions. Several neural cells, such as astrocytes, cerebellar granule neurons, neural stem cells and Schwann cells (SCs), have been proposed to convert BMSCs to a more committed neural fate (Song et al., 2002; Wisletgendebien et al., 2005; Zurita et al., 2005; Chen et al., 2006). Our group has shown that SCs can induce BMSCs to differentiate into neurons *in vitro*, and co-transplantation of both cells can promote functional recovery after spinal cord injury *in vivo* (Ban et al., 2011). Thus, it is necessary to explore potential mechanisms underlying this process of differentiation.

Signaling pathways for BMSC differentiation towards neuronal phenotypes include Wnt (Jing et al., 2015), PI3K (Kumar et al., 2015), HIF-1, and ROCK pathways (Pacary et al., 2007). In addition, recent studies have revealed that microRNAs (miRNAs) play key roles in the regulation of neuronal development and differentiation (Eda and Tamura, 2009; Perruisseaucarrier et al., 2011; Liu et al., 2012a). For example, increasing miR-124 expression can promote proliferation and differentiation of neuronal stem cells by inactivating the Notch pathway (Jiao et al., 2017). For BMSCs, miR-29a, miR-9, and miRNA let-7f-5p were shown to act as key regulators for neuronal differentiation (Jing et al., 2011; Duan et al., 2014; Han et al., 2018). However, no comprehensive miRNA analysis of BMSC neuronal differentiation under SC induction has been performed.

This study explored changes in miRNAs of BMSCs induced with SC-conditioned medium. The results will be helpful to establish a deeper understanding of underlying mechanisms and find novel strategies for cell therapy.

Materials and Methods

Animals

Twenty female Wistar rats aged 4-weeks-old and weighing 100 ± 10 g were obtained from Experimental Animal Center of the Academy of Military Medical Sciences, Beijing, China [License No. SYXK (Jin) 2014-0002]. Rats were kept in a humidity- and temperature-controlled environment with a 12-hour light-dark cycle. All protocols were approved by the Animal Ethics Committee of Institute of Radiation Medicine, Chinese Academy of Medical Sciences on March 12, 2017 (approval number: DWLI-20170311).

Culture of primary rat BMSCs

BMSCs were isolated from femoral and tibia bones in adult Wistar rats as previously described. Briefly, after anesthesia, bilateral femoral and tibia bones were carefully removed, both ends of bones were cut off, and the medullary cavity was rinsed with Dulbecco's Modified Eagle's Medium (DMEM; Gibco, Carlsbad, CA, USA) using a syringe. The flushed solution was collected and centrifuged at 300 × *g* for 3 minutes. Afterwards, resuspended cells were seeded in culture dishes containing complete medium [DMEM supplemented with 10% fetal bovine serum, 100 U/mL penicillin, and 100 μg/mL streptomycin (all from Gibco)]. After 48 hours of incubation, hematopoietic and other non-adherent cells were removed. Cells were digested with 0.25% trypsin (Sigma, Shanghai, China), collected, centrifuged, and expanded until passage 3 for characterization and differentiation experiments. BMSCs were characterized using flow cytometry with antibodies against CD34 (ab187284, mouse monoclonal; Abcam, Cambridge, UK), CD45 (202214, mouse monoclonal; BioLegend, San Diego, CA, USA), CD29 (102216, Armenian hamster monoclonal; BioLegend), and CD90 (206105, mouse monoclonal; BioLegend). Flow cytometry analysis was performed using a fluorescence-activated cell sorter (FACSCalibur; Becton Dickinson, San Jose, CA, USA) with the CELL Quest program (Becton Dickinson). A CytoFLEX instrument (Beckman Coulter, Shanghai, China) was used for flow cytometry.

Culture of SCs from rats and immunofluorescence staining

SCs were isolated and cultured according to previously modified protocols (Fan et al., 2017). The bilateral saphenous nerves of rats were removed after anesthesia. The epineurium was carefully stripped and the nerve tissue was cut into pieces, which were placed in pre-warmed trypsin (0.3%) for 30 minutes. Digested tissue was seeded in culture dishes containing complete medium (described above). Cells were incubated at 37°C in 5% CO_2 for 72 hours. Upon reaching 85% confluence, cells were passaged, and differential adherence was used for cell purification. Cells were passaged to passage 5 for further study. For identification of SCs, cells

were seeded on cover slips for 48 hours and then fixed by 4% paraformaldehyde for 15 minutes. After cells were permeabilized using Triton X-100 and blocked with 5% goat serum albumin for 1 hour, they were incubated with a primary S100 antibody (rabbit polyclonal, 1:100; Abcam) at 4°C overnight. After excess antibody was removed by rinsing with phosphate-buffered saline containing Tween 20, a secondary antibody (goat anti-rabbit IgG/FITC; 1:100; Sigma, St. Louis, MO, USA) was added and incubated for 2 hours at room temperature. Cell nuclei were stained by 4′,6-diamidine-2′-phenylindole dihydrochloride (DAPI, Abcam). Images were acquired with a fluorescence microscope (IX71, Olympus, Tokyo, Japan). Three slides were randomly selected, and ten fields were randomly selected from the three slides. Number of SCs was equal to (the number of S100-positive cells/the number of DAPI-positive cells) × 100%. Finally, the mean of S100 immunopositive ratios was calculated.

Neuronal differentiation of BMSCs with SC co-culture system

For induction of BMSC neuronal differentiation, BMSCs were cultured in SC-conditioned medium. BMSCs at P3–5 were used for experiments. Before induction, BMSCs were implanted onto coverslips at 3×10^4 cells per cm^2. SCs were cultured in other culture flasks at 1×10^5 cells/cm^2. SC-conditioned medium was collected and BMSCs medium was half-changed with SC-conditioned medium every day. The medium of control BMSCs was half-changed with complete medium. Changes in BMSC morphology were observed using time-lapse video microscopy (BioStation, Nikon, Japan) for 3 days.

Reverse transcription-polymerase chain reaction (RT-PCR) analysis

To analyze relative mRNA expression associated with neural markers in BMSCs, RT-PCR was employed. Expression levels of nestin, microtubule-associated protein 2 (MAP2) (Hashemi et al., 2017), tafazzin (Zhou et al., 2016), and protein phosphatase 1 (PP1C) (Fang et al., 2018) were normalized to the expression level of β-actin (Brett et al., 2011) (**Table 1**). Total RNA was isolated using a RiboPure™ RNA purification kit (AM1924; Thermo Fisher Scientific, Waltham, MA, USA), and 2.0 μg of total RNA was reverse-transcribed into cDNA using a high-capacity cDNA reverse transcription kit (4368814, Thermo Fisher Scientific). Fast Start Universal SYBR Green Master (Rox) was used for PCR reactions (7 μL ddH_2O, 1 μL cDNA, 1 μL forward primer, 1 μL reverse primer, and 10 μL SYBR qPCR Mix). All PCR reactions had three replicates. PCR reactions were performed as follows: 95°C for 30 seconds, then 40 cycles of 95°C for 5 seconds and 60°C for 30 seconds. All data were analyzed with the $2^{-\Delta\Delta Ct}$ method (Livak and Schmittgen, 2001). $P < 0.05$ was considered to indicate a statistically significant difference.

Table 1 Primers for reverse transcription-polymerase chain reaction

Gene	Sequence (5′–3′)	Product size (bp)
β-Actin	Forward: TGT TAC CAA CTG GGA CGA CA Reverse: CTC TCA GCT GTG GTG GTG AA	393
Nestin	Forward: CCT CAA GAT GTC CCT TAG TCT G Reverse: TCC AGA AAG CCA AGA GAA GC	114
MAP2	Forward: CAA ACG TCA TTA CTT TAC AAC TTG A Reverse: CAG CTG CCT CTG TGA GTG AG	122
TAZ	Forward: ATG TTG ACC TCG GGA CTT TGG Reverse: GAG GAA GGG CTC GCT TTT GT	89
PP1C	Forward: TTA GAC GTA TTA TGC GGC CC Reverse: GAG GAA GGG CTC GCT TTT GT	549

MAP2: Microtubule-associated protein 2; TAZ: tafazzin; PP1C: protein phosphatase 1.

MiRNA isolation and miRNA array

Total RNA from different groups was isolated for microRNA analyses using an RNeasy Mini kit (Qiagen, Hilden, Germany). Total RNA was quantified with a NanoDrop ND-2000 (Thermo Scientific), while an Agilent Bioanalyzer 2100 (Agilent Technologies, Santa Clara, CA, USA) was used to detect RNA integrity. An Agilent Rat miRNA (Release 21.0) chip was used in this study. According to the standard workflow for the chip, sample labeling, chip hybridization, and elution were conducted. An Agilent Scanner G2505C (Agilent Technologies) was used to scan the original image. Original data were processed using Feature Extraction software (version 10.7.1.1, Agilent Technologies). Genespring software (version 13.1, Agilent Technologies) was utilized to finish the quantile standardization and for subsequent processing. Differentially expressed miRNAs (DE-miRNAs) were screened *via* fold-change and *P* value of the applied *t*-test. Criteria applied in selected DE-miRNA were fold-change ≥ 2.0 and $P \leq 0.05$.

MiRNA target prediction, functional classification, and pathway analysis

Targetscan (http://www.targetscan.org), microRNA.org, and PITA (https://omictools.com/pita-tool) were used to predict target genes of DE-miRNAs. Gene Ontology (GO; http://geneontology.org) and Kyoto Encyclopedia of Genes and Genomes (KEGG; https://www.genome.jp/kegg/) pathway analyses were applied to determine roles of miRNA target genes with Cytoscape software 3.5.1 (http://www.cytoscape.org/). Hierarchical clustering was performed to show distinguishable miRNA expression patterns among samples. According to *P* values, the 15 most significant GO terms were selected for biological processes, cellular components, and molecular functions.

Statistical analysis

Data are expressed as the mean ± SD, and were analyzed using SPSS 13.0 software (SPSS Inc., Chicago, IL, USA). Statistical analysis was performed using two-sample *t* test and one-way analysis of variance followed by Tukey's *post hoc* test. All experiments were conducted at least three times. $P < 0.05$ was considered statistically significant.

Results

Identification of SCs and BMSCs

BMSCs were isolated from femoral and tibial bones of adult Wistar rats, and undifferentiated cells at P3–5 were examined

by flow cytometry for expression of surface markers (CD34, CD45, CD29, and CD90). BMSCs showed positive expression for CD29 and CD90 (**Figure 1A**). In contrast, BMSCs were clearly negative for hematopoietic markers CD34 and CD45 (**Figure 1B**). The bilateral saphenous nerves of rats were used to isolate SCs, and P3 cells were examined for SC identity using S-100/DAPI immunofluorescence staining. As shown in **Figure 1C**, the morphology of cells was almost spindle type, and 95.7 ± 0.8% of cells were positive for S100.

SC-conditioned medium induces BMSC differentiation into neuronal-like cells

SC-conditioned medium was used to induce differentiation of BMSCs into neuronal-like cells. The effect of SC-conditioned medium on BMSC differentiation was observed by time-lapse imaging (**Figure 1D–I**). The shape of BMSCs changed into neuronal-like cells, as the cell bodies of BMSCs gradually shrank and became bright, and several neurites formed. Furthermore, the inductive effects of SC-conditioned medium were detected by an increase in neuronal markers nestin and MAP2 (**Figure 1J**). Although nestin expression was present at 1, 3, 5, and 7 days in BMSCs with or without SC-conditioned medium, the results showed a notably higher amount of nestin in BMSCs induced with SC-conditioned medium compared with the BMSC control group at 3 days. However, nestin expression was reduced from 3 to 7 days. In contrast, expression of MAP2 was increased in BMSCs induced by SC-conditioned medium from 1 to 7 days compared with BMSCs without SC-conditioned medium (**Figure 1J**). Therefore, SC-medium promoted differentiation of BMSCs into neuronal-like cells.

Analysis of miRNA expression profile of BMSCs

MiRNA microarray was utilized to detect differentially expressed miRNAs (DE-miRNAs) in BMSCs cultured in unconditioned medium or with neural induction by SC-conditioned medium. DE-miRNAs were recognized according to the following criteria: upregulated or downregulated in the BMSC + SC group compared with the BMSC control group under the condition of "$P < 0.05$ and fold-change > 2.0". A total of 83 miRNAs were significantly differentially expressed, including 77 upregulated and 6 downregulated miRNAs. These DE-miRNAs were used to analyze target genes for further bioinformatic analyses (**Figure 2**).

Target gene prediction and ontology analysis of DE-miRNAs

The target genes of 83 DE-miRNAs were predicted using Targetscan, microRNA.org, and PITA. Subsequently, biological processes, cellular components, and molecular functions of DE-miRNA targets were analyzed through GO (**Figure 3**). With regard to biological processes, target genes for neuron projection development, regulation of axonogenesis, and positive regulation of cell proliferation were enriched (**Additional Table 1**). For cellular components, cytoplasm, plasma membrane, and membrane genes were enriched (**Additional Table 2**). For molecular functions, genes involved in protein binding, calcium ion binding, and ubiquitin protein ligase binding were enriched (**Additional Table 3**).

Pathway analysis of DE-miRNAs targets

KEGG pathway analysis was used to investigate potential pathways associated with neural differentiation (**Additional Table 4**). The results of pathway analysis showed that target genes were enriched in Hippo, Wnt, tumor growth factor-beta, and Hedgehog signaling pathways, which were potential acting pathways in neural differentiation of BMSCs (**Figure 4**).

Validation of DE-miRNA target gene expression

To validate the expression of DE-miRNA targets, RT-qPCR was utilized to detect the expression of tafazzin and PP1C. Tafazzin is involved in the Hippo signaling pathway, while PP1C is involved in the tumor growth factor-beta signaling pathway. After co-culture of BMSCs with SC-conditioned medium for 7 days, expression of tafazzin ($P < 0.0001$) and PP1C ($P < 0.001$) was downregulated in the BMSC + SC group compared with the BMSC control group (**Figure 5**).

Discussion

Neuronal differentiation of BMSCs has great potential for the treatment of various neurodegenerative disorders, such as Alzheimer's disease, Parkinson's disease, and brain/spinal cord injury (Shichinohe et al., 2015). Adoption of a co-culture strategy for clinical use avoids limitations associated with repeated exposure to chemical agents or neurotrophic factor injections. Paracrine factors secreted by supporting cells can modify not only the viability of transplanted cells, but also the rate of their neuronal differentiation. Numerous studies have shown that miRNAs play an important role in modulating neuronal differentiation of stem cells (Brett et al., 2011; Crobu et al., 2012; Stappert et al., 2013). In the current study, SCs induced BMSC differentiation into neuronal-like cells. Upon investigating the expression profile of miRNAs in BMSCs induced to differentiate into neuronal-like cells, and 83 DE-miRNAs were identified. The target genes of 15 DE-miRNAs were predicated, and potential acting pathways were examined.

KEGG analysis results showed that significantly changed miRNA targets were enriched in several neuronal differentiation pathways, including Hippo, Wnt, tumor growth factor-beta, and Hedgehog signaling pathways, which are described in more detail below.

Hippo signaling pathway

Hippo signaling is the key regulator in maintaining the self-renewal ability of stem cells, especially in the nervous system (Xiaomei et al., 2017). Yes-associated protein and its paralog tafazzin (transcriptional co-activator with PDZ-binding motif, also known as WW domain-containing transcription regulator 1, or Wwtr1) are the main downstream effectors of the Hippo signaling pathway (Guo and Teng, 2015). It has been demonstrated that Yes-associated protein/tafazzin-mediated nuclear accumulation of phosphoSmads is required for human embryonic stem cell plu-

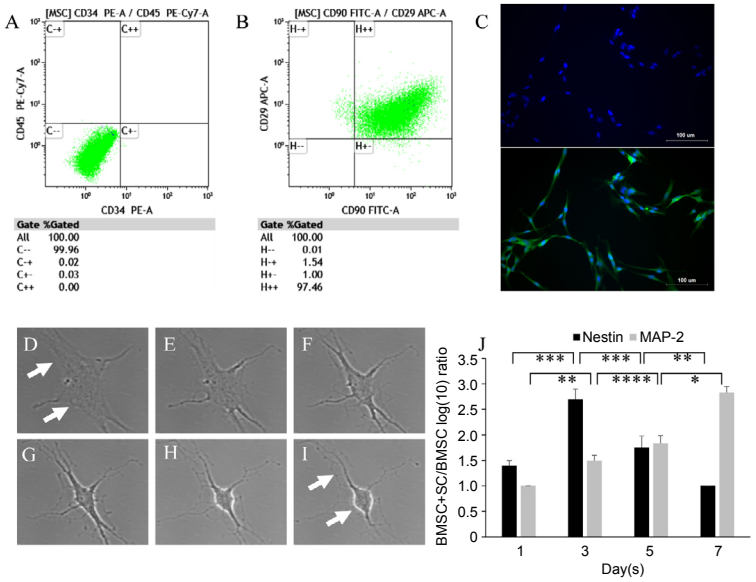

Figure 1 SCs induced differentiation of BMSCs into neuronal-like cells.

(A, B) Characterization of SCs and BMSCs: results of flow cytometry showed that cells expressed mesenchymal stem cell markers CD90 and CD29, but not hematopoietic markers CD34 or CD45. (C) Characterization of SCs with immunostaining of S100/DAPI. (D–I) Images of time-lapse imaging: changes of BMSCs into neuronal-like cells. Arrows mark the formation of neurites and changes in cell bodies. (J) Reverse transcription-polymerase chain reaction results: expression levels of nestin and MAP2 in BMSCs cultured in unconditioned or SC-conditioned medium (mean ± SD, n = 3; one-way analysis of variance followed by Turkey's *post hoc* test). $*P < 0.05$, $**P < 0.01$, $***P < 0.001$, $****P < 0.0001$. MAP2: Microtubule-associated protein 2; SCs: Schwann cells; BMSCs: bone marrow-derived mesenchymal stem cells.

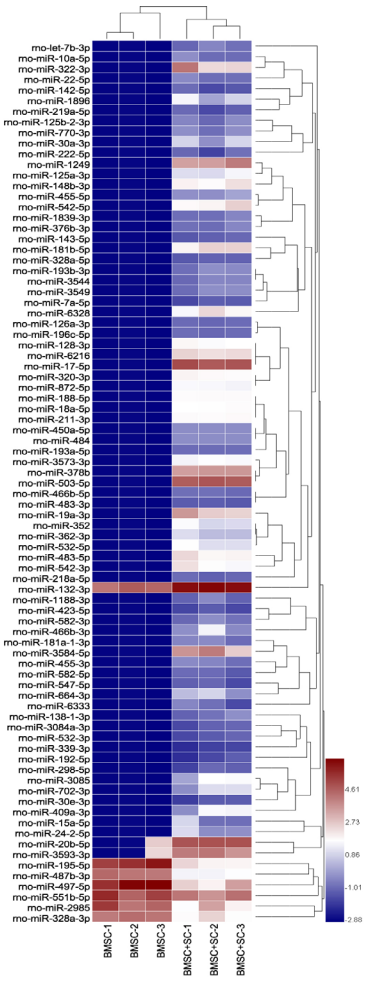

Figure 2 Heat map of miRNA expression levels in BMSCs.

miRNA microarray results from three replicates of two groups: BMSCs induced with SC-conditioned medium and BMSCs cultured in unconditioned medium. miRNA microarray results shown used hierarchal clustering of differentially expressed miRNA under the condition "$P < 0.05$ and fold change > 2.0". The rightmost legend represents fold-change. BMSCs: Bone marrow-derived mesenchymal stem cells; SC: Schwann cells.

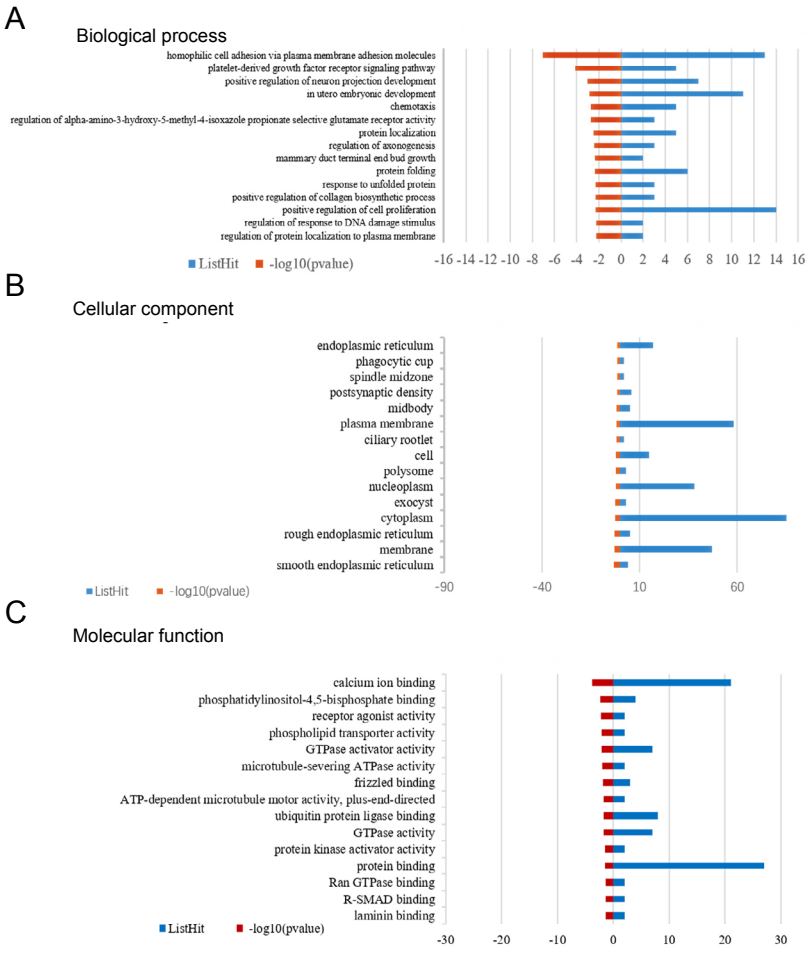

Figure 3 Gene Ontology (GO) analysis of biological process, cellular component, and molecular function.

The top 15 significant GO terms were listed for (A) biological processes, (B) cellular components, and (C) molecular functions. Blue column shows the number of genes, while red column shows the P value (–log10).

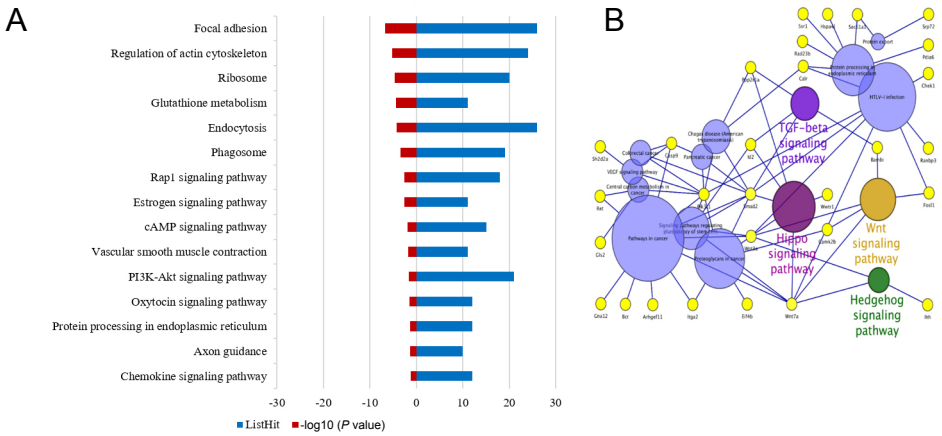

Figure 4 Pathway analysis of differentially expressed miRNA targets.
(A) KEGG pathway analysis results. Blue column shows the number of genes, while red column shows the *P* value (–log10). (B) Result generated by Cytoscape software 3.5.1. Circles representing TGF-beta, Hippo, Wnt, and Hedgehog signaling pathways are related to stem cell differentiation, while circles with different colors and the remaining yellow circles are not related. KEGG: Kyoto Encyclopedia of Genes and Genomes; TGF: transforming growth factor.

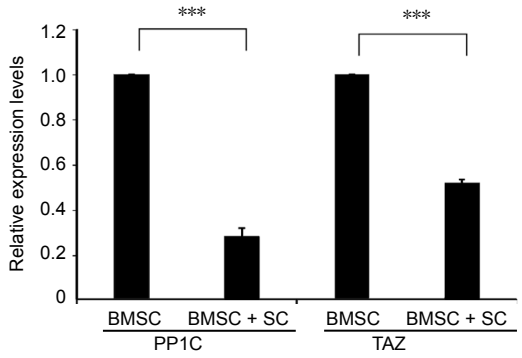

Figure 5 Validation of differentially expressed miRNA target genes.
Results of RT-PCR for TAZ and PP1C expression levels in BMSCs cultured with or without SC-conditioned medium (mean ± SD, $n = 3$; two-sample *t* test). ***$P < 0.001$. BMSCs: Bone marrow-derived mesenchymal stem cells; PP1C: protein phosphatase 1; SC: Schwann cell; TAZ: tafazzin.

ripotency (Varelas et al., 2008). Conversely, silencing of the Hippo signaling pathway results in neuroectoderm differentiation (Sun et al., 2014). Moreover, hypermethylation of Salvador/Warts/Hippo pathway genes can induce neuronal differentiation of BMSCs (Tzeng et al., 2015). In the current study, SC-induced neuronal differentiation of BMSCs led to obvious increases of miRNAs such as miR-17-5p, miR-20b-5p, and miR-503-5p, which all target tafazzin.

Wnt signaling pathway

Wnt signaling has an essential role in neuronal differentiation, nervous system development, synaptic maintenance, and neuronal functions (Arrázola et al., 2015; Inestrosa and Varelanallar, 2015). Multiple lines of evidence show that different stimuli can induce stem cells to differentiate into neuronal phenotypes by activating the Wnt signaling pathway (Liu et al., 2014; Chen et al., 2018; Grünblatt et al., 2018). miR-128-3p, which was upregulated in BMSCs induced by co-culture with SCs, is firmly associated with the Wnt signaling pathway. miR-128 can synergize with miR-124 and miR-137 to promote differentiation of neural stem cells (Santos et al., 2016). Moreover, miR-218 serves as a crucial constituent regulator of neuronal differentiation of adipose stem cells through the Wnt signaling pathway (Hu et al., 2017). miR-128 has also been used to induce neural differentiation of induced pluripotent stem cells (Zare et al., 2015).

Tumor growth factor-beta signaling pathway

The tumor growth factor-beta signaling pathway plays an important role in forming the neural tube and patterning the spinal cord, with tumor growth factor-beta family members exerting both positive and negative regulation of neuronal differentiation (Meyers and Kessler, 2017). Smad2, an important component of the tumor growth factor-beta signaling pathway, was shown to be a potential target of miR-455-3p in Alzheimer's disease postmortem brain (Kumar and Reddy, 2018). miR-10a and miR-195 also exhibited a relationship with tumor growth factor-beta signaling *via* different biological processes (Sun et al., 2015; Duan and Chen, 2016). Moreover, engrafted peripheral blood-derived MSCs could differentiate into central nervous system cells *via* increased expression of tumor growth factor-beta, which promoted locomotive recovery in adult rats after spinal cord injury (Fu et al., 2017).

Hedgehog signaling pathway

Sonic hedgehog (Shh) and its downstream signaling regulate the early induction and expansion of progenitors during central nervous system development (Feuerstein et al., 2017). In addition, Shh is one of the main motor neuron differentiation inducers in human pluripotent stem cells (Sun et al., 2014). miR-128, miR-195, and miR-503, which participate in Hippo, Wnt, and tumor growth factor-beta signaling pathways, were also enriched for the Shh signaling pathway. Numerous studies have implicated miRNAs as cellular switches that modulate cellular outcomes in response to regulation of signaling networks during stem cell differentiation, which is consistent with our current results (Aval et al., 2017).

The results of this study provide a miRNA profile of BMSCs differentiated into neuronal-like cells upon induction with SC-conditioned medium. Microarray and subsequent pathway analyses revealed key miRNAs and signaling path-

ways for neuronal differentiation of BMSCs. Although this experiment validated the expression of some genetic targets, it is still necessary to verify the function of target genes and implicated signaling pathways in future experiments.

Acknowledgments: *We are grateful for Professor Xiaohong Kong and Chang Liu from 221 Laboratory, School of Medicine, Nankai University, Tianjin, China for their valuable suggestions.*
Author contributions: *Study conception and design: SQF, ZJW, BYF , YL; experimental implementation: ZJW, BYF, YL; provision of critical reagents and scientific input: HD, HST, DYP; caring for rats: JXS, PYZ, HYS; data analysis: HW, AL, SQF; manuscript preparation: ZJW, BYF, YL. All authors approved the final version of the paper.*
Conflicts of interest: *The authors declare that there are no conflicts of interest associated with this manuscript.*
Financial support: *The present study was supported by the National Natural Science Foundation of China, No. 81330042, 81620108018, and 81702147 (both to ZJW). The funding sources had no role in study conception and design, data analysis or interpretation, paper writing or deciding to submit this paper for publication.*
Institutional review board statement: *All procedures were approved by the Animal Ethics Committee of Chinese Academy of Medical Sciences Institute of Radiation Medicine, China on March 12, 2017 (approval No. DWLI-20170311). All experimental procedures described here were in accordance with the National Institutes of Health (NIH) guidelines for the Care and Use of Laboratory Animals.*

Data sharing statement: *Datasets analyzed during the current study are available from the corresponding author on reasonable request.*
Plagiarism check: *Checked twice by iThenticate.*
Peer review: *Externally peer reviewed.*

Additional files:

Additional Table 1: *Biological process.*
Additional Table 2: *Cellular component.*
Additional Table 3: *Molecular function.*
Additional Table 4: *Kyoto Encyclopedia of Genes and Genomes.*

References

Arrázola MS, Silvaalvarez C, Inestrosa NC (2015) How the Wnt signaling pathway protects from neurodegeneration: the mitochondrial scenario. Front Cell Neurosci 9:166.

Aval SF, Lotfi H, Sheervalilou R, Zarghami N (2017) Tuning of major signaling networks (TGF-β, Wnt, Notch and Hedgehog) by miRNAs in human stem cells commitment to different lineages: possible clinical application. Retour Au Numéro 91:849.

Ban DX, Ning GZ, Feng SQ, Wang Y, Zhou XH, Liu Y, Chen JT (2011) Combination of activated Schwann cells with bone mesenchymal stem cells: the best cell strategy for repair after spinal cord injury in rats. Regen Med 6:707.

Bertani N, Malatesta P, Volpi G, Sonego P, Perris R (2005) Neurogenic potential of human mesenchymal stem cells revisited: analysis by immunostaining, time-lapse video and microarray. J Cell Sci 118:3925-3936.

Brett JO, Renault VM, Rafalski VA, Webb AE, Brunet A (2011) The microRNA cluster miR-106b~25 regulates adult neural stem/progenitor cell proliferation and neuronal differentiation. Aging (Albany NY) 3:108-124.

Chen X, Zhou B, Yan T, Wu H, Feng J, Chen H, Gao C, Peng T, Yang D, Shen J (2018) Peroxynitrite enhances self-renewal, proliferation and neuronal differentiation of neural stem/progenitor cells through activating HIF-1α and Wnt/β-catenin signaling pathway. Free Radic Biol Med 117:158-167.

Chen Y, Teng FY, Tang BL (2006) Coaxing bone marrow stromal mesenchymal stem cells towards neuronal differentiation: progress and uncertainties. Cell Mol Life Sci 63:1649.

Crobu F, Latini V, Marongiu MF, Sogos V, Scintu F, Porcu S, Casu C, Badiali M, Sanna A, Manchinu MF (2012) Differentiation of single cell derived human mesenchymal stem cells into cells with a neuronal phenotype: RNA and microRNA expression profile. Mol Biol Rep 39:3995-4007.

Deng W, Obrocka M, Fischer I, Prockop DJ (2001) In vitro differentiation of human marrow stromal cells into early progenitors of neural cells by conditions that increase intracellular cyclic AMP. Biochem Biophys Res Commun 282:148-152.

Duan P, Sun S, Li B, Huang C, Xu Y, Han X, Xing Y, Yan W (2014) miR-29a modulates neuronal differentiation through targeting REST in mesenchymal stem cells. PLoS One 9:e97684.

Duan Y, Chen Q (2016) TGF-β1 regulating miR-205/miR-195 expression affects the TGF-β signal pathway by respectively targeting SMAD2/SMAD7. Oncol Rep 36:1837-1844.

Eda A, Tamura YyM (2009) Systematic gene regulation involving miRNAs during neuronal differentiation of mouse P19 embryonic carcinoma cell. Biochem Biophys Res Commun 388:648-653.

Fan BY, Zhou XH, Wang LN, Wei ZJ, Lin W, Ren YM, Shi GD, Cheng X, Wang LY, Feng SQ (2017) In vitro study of neural stem cells and activated Schwann cells cocultured on electrospinning polycaprolactone scaffolds. J Neurorestoratol 5:155-165.

Fang HY, Hung MY, Lin YM, Pandey S, Chang CC, Lin KH, Shen CY, Viswanadha VP, Kuo WW, Huang CY (2018) 17β-Estradiol and/or estrogen receptor alpha signaling blocks protein phosphatase 1 mediated ISO induced cardiac hypertrophy. PLoS One 13:e0196569.

Feuerstein M, Chleilat E, Khakipoor S, Michailidis K, Ophoven C, Roussa E (2017) Expression patterns of key Sonic Hedgehog signaling pathway components in the developing and adult mouse midbrain and in the MN9D cell line. Cell Tissue Res 370:211-225.

Fu Q, Liu Y, Liu X, Zhang Q, Chen L, Peng J, Ao J, Li Y, Wang S, Song G (2017) Engrafted peripheral blood-derived mesenchymal stem cells promote locomotive recovery in adult rats after spinal cord injury. Am J Transl Res 9:3950.

Garg M, Kaur S, Banik A, Kumar V, Rastogi A, Sarin SK, Mukhopadhyay A, Trehanpati N (2017) Bone marrow endothelial progenitor cells activate hepatic stellate cells and aggravate carbon tetrachloride induced liver fibrosis in mice via paracrine factors. Cell Prolif 50:e12355.

Grünblatt E, Bartl J, Walitza S (2018) Methylphenidate enhances neuronal differentiation and reduces proliferation concomitant to activation of Wnt signal transduction pathways. Transl Psychiatry 8:51.

Guo L, Teng L (2015) YAP/TAZ for cancer therapy: opportunities and challenges (review). Int J Oncol 46:1444.

Han L, Wang Y, Wang L, Guo B, Pei S, Jia Y (2018) MicroRNA let-7f-5p regulates neuronal differentiation of rat bone marrow mesenchymal stem cells by targeting Par6α. Biochem Biophys Res Commun 495:1476-1481.

Hashemi E, Sadeghi Y, Aliaghaei A, Seddighi A, Piryaei A, Broujeni ME, Shaerzadeh F, Amini A, Pouriran R (2017) Neural differentiation of choroid plexus epithelial cells: role of human traumatic cerebrospinal fluid. Neural Regen Res 12:84.

Hu F, Sun B, Xu P, Zhu Y, Meng XH, Teng GJ, Xiao ZD (2017) MiR-218 induces neuronal differentiation of ASCs in a temporally sequential manner with fibroblast growth factor by regulation of the wnt signaling pathway. Sci Rep 7:39427.

Hung S, Cheng H, Pan C, Tsai M, Kao L, Ma H (2002) In vitro differentiation of size-sieved stem cells into electrically active neural cells. Stem Cells 20:522.

Inestrosa NC, Varelanallar L (2015) Wnt signalling in neuronal differentiation and development. Cell Tissue Res 359:215-223.

Jiao S, Liu Y, Yao Y, Teng J (2017) miR-124 promotes proliferation and differentiation of neuronal stem cells through inactivating Notch pathway. Cell Biosci 7:68.

Jing L, Jia Y, Lu J, Han R, Li J, Wang S, Peng T, Jia Y (2011) MicroRNA-9 promotes differentiation of mouse bone mesenchymal stem cells into neurons by Notch signaling. Neuroreport 22:206-211.

Jing Y, Zhang JC, Su-Ting LI, Zhao JH, Wang J, Han XF, Xing Y (2015) Wnt/β-catenin pathway might underlie the MET in trans-differentiation from MSC to MSC-derived neuron. Zhongguo Yingyong Shenglixue Zahzi 31:572.

Kumar A, Mishra HK, Dwivedi P, Subramaniam JR (2015) Secreted trophic factors of human umbilical cord stromal cells induce differentiation and neurite extension through PI3K and independent of cAMP pathway. Ann Neurosci 22:97.

Kumar S, Reddy PH (2018) MicroRNA-455-3p as a potential biomarker for Alzheimer's disease: an update. Front Aging Neurosci 10:41.

Liu J, Githinji J, McLaughlin B, Wilczek K, Nolta J (2012) Role of miRNAs in neuronal differentiation from human embryonic stem cell-derived neural stem cells. Stem Cell Rev 8:1129-1137.

Liu M, Guo J, Wang J, Zhang L, Pang T, Liao H (2014) Bilobalide induces neuronal differentiation of P19 embryonic carcinoma cells via activating Wnt/β-catenin pathway. Cell Mol Neurobiol 34:913-923.

Livak KJ, Schmittgen TD (2001) Analysis of relative gene expression data using real-time quantitative PCR and the 2(-Delta Delta C(T)) Method. Methods 25:402-408.

Meyers EA, Kessler JA (2017) TGF-β family signaling in neural and neuronal differentiation, development, and function. Cold Spring Harb Perspect Biol 137:63-69.

Neuhuber B, Gallo G, Howard L, Kostura L, Mackay A, Fischer I (2004) Reevaluation of in vitro differentiation protocols for bone marrow stromal cells: disruption of actin cytoskeleton induces rapid morphological changes and mimics neuronal phenotype. J Neurosci Res 77:192-204.

Pacary E, Tixier E, Coulet F, Roussel S, Petit E, Bernaudin M (2007) Crosstalk between HIF-1 and ROCK pathways in neuronal differentiation of mesenchymal stem cells, neurospheres and in PC12 neurite outgrowth. Mol Cell Neurosci 35:409-423.

Perruisseaucarrier C, Jurga M, Forraz N, Mcguckin CP (2011) miRNAs stem cell reprogramming for neuronal induction and differentiation. Mol Neurobiol 43:215-227.

Robey P (2017) "Mesenchymal stem cells": fact or fiction, and implications in their therapeutic use. F1000Res 6:524.

Santos MCT, Tegge AN, Correa BR, Mahesula S, Kohnke LQ, Qiao M, Ferreira MAR, Kokovay E, Penalva LOF (2016) miR-124, -128, and -137 orchestrate neural differentiation by acting on overlapping gene sets containing a highly connected transcription factor network. Stem Cells 34:220-232.

Schultz SS, Lucas PA (2006) Human stem cells isolated from adult skeletal muscle differentiate into neural phenotypes. J Neurosci Methods 152:144-155.

Seo N, Lee SH, Ju KW, Woo J, Kim B, Kim S, Jahng JW, Lee JH (2018) Low-frequency pulsed electromagnetic field pretreated bone marrow-derived mesenchymal stem cells promote the regeneration of crush-injured rat mental nerve. Neural Regen Res 13:145-153.

Shichinohe H, Ishihara T, Takahashi K, Tanaka Y, Miyamoto M, Yamauchi T, Saito H, Takemoto H, Houkin K, Kuroda S (2015) Bone marrow stromal cells rescue ischemic brain by trophic effects and phenotypic change toward neural cells. Neurorehabil Neural Repair 29:80.

Song H, Stevens CF, Gage FH (2002) Astroglia induce neurogenesis from adult neural stem cells. Nature 417:39-44.

Song S, Song S, Zhang H, Cuevas J, Sanchez-Ramos J (2007) Comparison of neuron-like cells derived from bone marrow stem cells to those differentiated from adult brain neural stem cells. Stem Cells Dev 16:747-756.

Stappert L, Borghese L, Roese-Koerner B, Weinhold S, Koch P, Terstegge S, Uhrberg M, Wernet P, Brüstle O (2013) MicroRNA-based promotion of human neuronal differentiation and subtype specification. PLoS One 8:e59011.

Sun W, Ma Y, Chen P, Wang D (2015) MicroRNA-10a silencing reverses cisplatin resistance in the A549/cisplatin human lung cancer cell line via the transforming growth factor-β/Smad2/STAT3/STAT5 pathway. Mol Med Rep 11:3854-3859.

Sun Y, Yong KM, Villa-Diaz LG, Zhang X, Chen W, Philson R, Weng S, Xu H, Krebsbach PH, Fu J (2014) Hippo/YAP-mediated rigidity-dependent motor neuron differentiation of human pluripotent stem cells. Nat Mater 13:599-604.

Tohill M, Mantovani C, Wiberg M, Terenghi G (2004) Rat bone marrow mesenchymal stem cells express glial markers and stimulate nerve regeneration. Neurosci Lett 362:200-203.

Tzeng HH, Hsu CH, Chung TH, Lee WC, Lin CH, Wang WC, Hsiao CY, Leu YW, Wang TH (2015) Cell signaling and differential protein expression in neuronal differentiation of bone marrow mesenchymal stem cells with hypermethylated Salvador/Warts/Hippo (SWH) pathway genes. PLoS One 10:e0145542.

Tzeng SF, Tsai MJ, Hung SC, Cheng H (2004) Neuronal morphological change of size-sieved stem cells induced by neurotrophic stimuli. Neurosci Lett 367:23-28.

Vaquero J, Zurita M (2011) Functional recovery after severe CNS trauma: current perspectives for cell therapy with bone marrow stromal cells. Prog Neurobiol 93:341-349.

Varelas X, Sakuma R, Samavarchitehrani P, Peerani R, Rao BM, Dembowy J, Yaffe MB, Zandstra PW, Wrana JL (2008) TAZ controls Smad nucleocytoplasmic shuttling and regulates human embryonic stem-cell self-renewal. Nat Cell Biol 10:837-848.

Venkatesh K, Sen D (2016) Mesenchymal stem cells as a source of dopaminergic neurons: a potential cell based therapy for Parkinson's disease. Curr Stem Cell Res Ther 12:326-347.

Wiegner R, Rudhart NE, Barth E, Gebhard F, Lampl L, Huber-Lang MS, Brenner RE (2017) Mesenchymal stem cells in peripheral blood of severely injured patients. Eur J Trauma Emerg Surg 44:627-636.

Wisletgendebien S, Hans G, Leprince P, Rigo JM, Moonen G, Rogister B (2005) Plasticity of cultured mesenchymal stem cells: switch from nestin-positive to excitable neuron-like phenotype. Stem Cells 23:392-402.

Woodbury D, Reynolds K, Black IB (2002) Adult bone marrow stromal stem cells express germline, ectodermal, endodermal, and mesodermal genes prior to neurogenesis. J Neurosci Res 69:908-917.

Woodbury D, Schwarz EJ, Prockop DJ, Black IB (2000) Adult rat and human bone marrow stromal cells differentiate into neurons. J Neurosci Res 61:364-370.

Xiaomei B, Qing H, Ying W, Zhihui H, Zengqiang Y (2017) The roles and mechanisms of the Hippo/YAP signaling pathway in the nervous system. Hereditas 39:630-641.

Xu LL, Wang HY, Li XD, Liu B, Zheng FF, Yang NL (2017) Comparison of three kinds of mesenchymal stem cells differentiating into nerve cells under co-culture induction. Zhongguo Zuzhi Gongcheng Yanjiu 21:2714-2721.

Yang Y, Xu Q, Wang HL, Yao MX (2018) Three kinds of mesenchymal stem cells:differentiating into neuron-like cells. Zhongguo Zuzhi GongchengYanjiu 22:5356-5361.

Zare M, Soleimani M, Akbarzadeh A, Bakhshandeh B, Aghaee-Bakhtiari SH, Zarghami N (2015) A novel protocol to differentiate induced pluripotent stem cells by neuronal microRNAs to provide a suitable cellular model. Chem Biol Drug Des 86:232-238.

Zhou J, Wei F, Ma Y (2016) Inhibiting PPARγ by erythropoietin while upregulating TAZ by IGF1 synergistically promote osteogenic differentiation of mesenchymal stem cells. Biochem Biophys Res Commun 478:349-355.

Zurita M, Bonilla C, Otero L, Aguayo C, Vaquero J (2008) Neural transdifferentiation of bone marrow stromal cells obtained by chemical agents is a short-time reversible phenomenon. Neurosci Res 60:275-280.

Zurita M, Vaquero J, Oya S, Miguel M (2005) Schwann cells induce neuronal differentiation of bone marrow stromal cells. Neuroreport 16:505-508.

C-Editor: Zhao M; S-Editors: Wang J, Li CH; L-Editors: Deusen AV, Raye W, Qiu Y, Song LP; T-Editor: Liu XL

Additional Table 1 Biological process

Term_ID	Term_description	*P*-value	FDR_bh
GO:0007156	homophilic cell adhesion via plasma membrane adhesion molecules	8.70E-08	8.98E-05
GO:0048008	platelet-derived growth factor receptor signaling pathway	7.83E-05	0.04039946
GO:0010976	positive regulation of neuron projection development	0.000946	0.30513523
GO:0001701	in utero embryonic development	0.001445	0.30513523
GO:0006935	chemotaxis	0.001786	0.30513523
GO:2000311	regulation of alpha-amino-3-hydroxy-5-methyl-4-isoxazole propionate selective glutamate receptor activity	0.002013	0.30513523
GO:0008104	protein localization	0.003263	0.30513523
GO:0050770	regulation of axonogenesis	0.003875	0.30513523
GO:0060763	mammary duct terminal end bud growth	0.004348	0.30513523
GO:0006457	protein folding	0.004496	0.30513523
GO:0032967	positive regulation of collagen biosynthetic process	0.004836	0.30513523
GO:0006986	response to unfolded protein	0.004836	0.30513523
GO:0008284	positive regulation of cell proliferation	0.004888	0.30513523
GO:1903076	regulation of protein localization to plasma membrane	0.005543	0.30513523
GO:2001020	regulation of response to DNA damage stimulus	0.005543	0.30513523

Additional Table 2 Cellular component

Term_ID	Term_description	*P*-value	FDR_bh
GO:0005790	smooth endoplasmic reticulum	0.000755	0.114446
GO:0016020	membrane	0.001475	0.114446
GO:0005791	rough endoplasmic reticulum	0.001677	0.114446
GO:0005737	cytoplasm	0.002674	0.114446
GO:0000145	exocyst	0.002791	0.114446
GO:0005654	nucleoplasm	0.00541	0.184856
GO:0005844	polysome	0.011325	0.253304
GO:0005623	cell	0.011548	0.253304
GO:0035253	ciliary rootlet	0.011969	0.253304
GO:0005886	plasma membrane	0.012356	0.253304
GO:0030496	midbody	0.020394	0.380062
GO:0014069	postsynaptic density	0.027171	0.39995
GO:0051233	spindle midzone	0.027468	0.39995
GO:0001891	phagocytic cup	0.027468	0.39995
GO:0005783	endoplasmic reticulum	0.029265	0.39995

Additional Table 3 Molecular function

Term_ID	Term_description	*P*-value	FDR_bh
GO:0005509	calcium ion binding	0.000154	0.043551
GO:0005546	phosphatidylinositol-4,5-bisphosphate binding	0.004374	0.424995
GO:0048018	receptor agonist activity	0.006607	0.424995
GO:0005548	phospholipid transporter activity	0.008009	0.424995
GO:0005096	GTPase activator activity	0.008206	0.424995
GO:0008568	microtubule-severing ATPase activity	0.011173	0.424995
GO:0005109	frizzled binding	0.013705	0.424995
GO:0008574	ATP-dependent microtubule motor activity, plus-end-directed	0.018851	0.424995
GO:0031625	ubiquitin protein ligase binding	0.019378	0.424995
GO:0003924	GTPase activity	0.019937	0.424995
GO:0030295	protein kinase activator activity	0.036129	0.424995
GO:0005515	protein binding	0.038027	0.424995
GO:0070412	R-SMAD binding	0.038952	0.424995
GO:0008536	Ran GTPase binding	0.038952	0.424995
GO:0043236	laminin binding	0.047898	0.424995

Additional Table 4 Kyoto Encyclopedia of Genes and Genomes

Term_ID	Term_description	*P*-value	FDR_bh
path:rno04390	Hippo signaling pathway	0.013758	0.539976
path:rno05205	Proteoglycans in cancer	0.014034	0.539976
path:rno04141	Protein processing in endoplasmic reticulum	0.018949	0.539976
path:rno04350	TGF-beta signaling pathway	0.021136	0.539976
path:rno04340	Hedgehog signaling pathway	0.023754	0.539976
path:rno05200	Pathways in cancer	0.026558	0.539976
path:rno05166	HTLV-I infection	0.030002	0.539976
path:rno04550	Signaling pathways regulating pluripotency of stem cells	0.032952	0.539976
path:rno04310	Wnt signaling pathway	0.033787	0.539976
path:rno04370	VEGF signaling pathway	0.040848	0.539976
path:rno03060	Protein export	0.044976	0.539976
path:rno05142	Chagas disease (American trypanosomiasis)	0.045752	0.539976
path:rno05210	Colorectal cancer	0.047615	0.539976
path:rno05230	Central carbon metabolism in cancer	0.049388	0.539976
path:rno05212	Pancreatic cancer	0.049388	0.539976